NEOPLASIA
www.neoplasia.com

Volume 11 Number 7 July 2009 pp. 651–661 651

CXCR4 Regulates the Early Extravasation of Metastatic Tumor Cells *In Vivo*[1,2]

Peter Gassmann*, Jörg Haier*, Kerstin Schlüter*, Britta Domikowsky*, Claudia Wendel*, Ulrike Wiesner†, Robert Kubitza†, Rainer Engers‡, Stephan W. Schneider§, Bernhard Homey† and Anja Müller¶

*Department of General and Visceral Surgery, University Hospital Muenster, Muenster, Germany; †Department of Dermatology, University Hospital Duesseldorf, Duesseldorf, Germany; ‡Department of Pathology, University Hospital Duesseldorf, Duesseldorf, Germany; §Department of Dermatology, University Hospital Muenster, Muenster, Germany; ¶Department of Radiation Oncology, University Hospital Duesseldorf, Duesseldorf, Germany

Abstract

Recent studies have demonstrated that the chemokine receptor CXCR4 plays a crucial role in organ-specific metastasis formation. Although a variety of studies showed the expression of chemokine receptors, in particular, CXCR4, by gastrointestinal tumors, the precise mechanisms of chemokine receptor–mediated homing of cancer cells to specific sites of metastasis remained elusive. Here, we used liver metastatic human HEP-G2 hepatoma and HT-29LMM colon cancer cells expressing functional CXCR4 to dissect the metastatic cascade by intravital fluorescence microscopy. Immunohistochemistry revealed that the CXCR4 ligand CXCL12 is expressed by endothelial cells and likely Kupffer cells lining the liver sinusoids. Tumor cell adhesion and extravasation *in vivo* was quantitatively analyzed using intravital fluorescence microscopy. Treatment of cells with an anti-CXCR4 antibody did not affect cell adhesion but significantly impaired tumor cell extravasation (HEP-G2; isotype control: 22.3% ± 4.3% *vs* anti-CXCR4: 6.0% ± 5.0%, $P < .001$). In addition, pretreatment of tumor cells with the ligand CXCL12 enhanced the activation of the small GTPases Rho, Rac, and cdc42 as well as tumor cell extravasation without affecting tumor cell adhesion within liver sinusoids. Taken together, the findings of the present study provide first *in vivo* insights into the early events of chemokine ligand/receptor–mediated liver metastasis formation of tumor cells and define tumor cell extravasation rather than tumor cell arrest as the rate-limiting event.

Neoplasia (2009) 11, 651–661

Introduction

The occurrence of metastases within distant organs represents the life-threatening event that limits the survival of patients with malignant diseases. To form clinically evident metastases, tumor cells have to complete a series of highly regulated steps. This metastatic cascade is initiated by local invasion and intravasation of tumor cells at the primary site, their subsequent adhesion/arrest is within vessels of target organs, and is followed by cell migration, leading to the extravasation of tumor cells [1]. Within target organs, the survival, promotion of tumor cell growth, and the induction of neoangiogenesis complete the series of steps finally resulting in successful formation of metastatic foci [2].

Abbreviations: ECM, extracellular matrix; HUVEC, human umbilical vein endothelial cell

Address all correspondence to: Peter Gassmann, MD, Department of General and Visceral Surgery, University Hospital Muenster, Waldeyerstrasse 1, D-48149 Muenster, Germany. E-mail: Peter.Gassmann@ukmuenster.de

[1]A.M. and B.H. are funded by the "Deutsche Krebshilfe" (10-2043-Mü I/II) and "Deutsche Forschungsgemeinschaft" SPP 1190 (Ho 2011/4-1). There are no commercial affiliations or financial interests that may be considered conflict of interests regarding the presented results by any author.

[2]This article refers to supplementary materials, which are designated by Tables W1 and W2 and are available online at www.neoplasia.com.

Received 3 February 2009; Revised 31 March 2009; Accepted 2 April 2009

DOI 10.1593/neo.09272

Notably, the early steps of metastasis seem to mimic, in part, events underlying leukocyte trafficking. Recent findings demonstrate that chemokine ligand/receptor interactions critically regulate the firm adhesion of distinct leukocyte subsets to the endothelium and mediate their transendothelial migration [3,4]. Subsequently, tumor cells of various origin have been shown to express distinct patterns of chemokine receptors mediating tumor cell migration, invasion, proliferation, and survival *in vitro* [5–8]. *In vivo*, the overexpression of distinct chemokine receptors on tumor cells, in particular, CXCR4, was enhanced, whereas their neutralization significantly impaired the formation of metastases [9–12]. In clinical studies, the overexpression of the chemokine receptor CXCR4 was associated with an impaired prognosis of patients undergoing surgery for colorectal liver metastasis [13]. In patients with hepatocellular carcinoma, higher levels of CXCR4 expression were associated with advanced local tumor progression, metastatic dissemination, and poor outcome [14]. Although their role in organ-specific metastasis formation is established, the underlying mechanisms of chemokine receptor–mediated dissemination of tumor cells remain elusive.

In the present study, we sought to dissect the steps of chemokine receptor–mediated events during early phases of metastasis *in vivo*. Therefore, the interaction of tumor cells with the microvessel system of the liver, as one major metastatic target organ, was analyzed using intravital fluorescence microscopy [15,16].

Materials and Methods

Cell Lines and Tissue Specimens

Human Caco-2 (ATCC, Wesel, Germany), HT-29LMM, and HT-29P (I. Fidler, Houston, TX) colorectal carcinoma cells and human HEP-G2 hepatocellular carcinoma cells (ATCC) were cultured in RPMI 1640 medium (GIBCO-BRL, Karlsruhe, Germany) containing 10% fetal bovine serum (GIBCO) or minimum essential medium alpha medium (GIBCO) containing 20% fetal bovine serum, respectively. Semiconfluent cells were cultured and prepared as previously described [17]. After trypsination, cell surface proteins were reconstituted in serum-free medium containing 1% bovine serum albumin (BSA; Sigma, Deisenhofen, Germany) before using in all experiments.

Human tissue specimens were taken from surgical specimens after obtaining informed consent from patients and were routinely fixed in 3.7% formalin and paraffin-embedded.

Immunohistochemistry

Paraffin sections from human colorectal carcinomas and liver metastases from colorectal carcinomas were immunohistochemically stained for CXCR4 expression as previously described [9].

For the detection of CXCL12 expression, sections of paraffin-embedded normal human liver samples (n = 10) were fixed and deparaffinized. Antigens were unmasked using the DakoCytomation Target Retrieval (Dako, Hamburg, Germany) and a high-pressure cooker followed by H_2O_2 treatment and an avidin and biotin blocking step (Blocking Kit; Vector, Burlingame, CA). Sections were stained with monoclonal antibodies directed against human CXCL12 (mouse immunoglobulin G1 [IgG1], 79018.111; R&D Systems, Minneapolis, MN) or isotype control antibodies (R&D Systems). Development of the staining was performed with the Vectastain ABC and AEC kits (Vector). Sections were counterstained with hematoxylin.

Quantitative Real-time Reverse Transcription–Polymerase Chain Reaction (TaqMan)

Total RNA of tumor cells was extracted (TRIzol reagent, Invitrogen, Carlsbad, CA), DNase-treated, and reverse-transcribed as described previously [9,18]. Complementary DNA (cDNA) was quantitatively analyzed for the expression of human chemokines and chemokine receptors by the fluorogenic 5′-nuclease polymerase chain reaction (PCR) assay as reported [9,18]. Specific primers and probes were obtained from Applied Biosystems (Foster City, CA). Gene-specific PCR products were continuously measured during 40 cycles with the ABI PRISM 7000 Sequence Detection System (Applied Biosystems). Quantitative real-time reverse transcription–PCR (RT-PCR) was performed with SYBR green as reporter for reactions using chemokine receptor–specific primers and 6-carboxylfluorescein as reporter for reactions using chemokine receptor–specific primer/probe combinations. Probes for the internal positive control (ribosomal 18S RNA) were associated with the VIC reporter. Target gene expression was normalized between different samples based on the values of ribosomal 18S RNA expression. Plasmid cDNA for chemokine receptors were used for quantification of target gene-specific messenger RNA (mRNA) expression.

Flow Cytometric Analysis of Chemokine Receptors and Integrin Expression

Flow cytometric analysis of chemokine receptor expression was performed as previously described [9]. Alternatively, cells were permeabilized for intracellular staining by incubating with methanol. For flow cytometric analysis of integrin expression, cells were trypsinized and washed in serum-free medium. After reconstitution for 60 minutes, cells were fixed with fresh 1% paraformaldehyde. Cells were then processed as described for CXCR4 detection. The following antibodies were used: anti–human integrin β_1 monoclonal antibody (mAb, clone P4C10; Chemicon, Hofheim, Germany), anti–human integrin β_4 mAb (clone ASC-8; Chemicon), anti–human integrin β_3 (clone N-20; Santa Cruz, Heidelberg, Germany), anti–human α_v mAb (clone 272-17E6; Calbiochem, Darmstadt, Germany), anti–human α_1 integrin mAb (clone SP2/0; Upstate, Lake Placid, NY), anti–human α_2 integrin mAb (clone 16B4; Serotec, Oxford, United Kingdom), anti–human α_3 integrin mAb (clone ASC-1; Chemicon), anti–human α_4 integrin mAb (kindly provided by J. Eble, Muenster), anti–human α_5 mAb (clone JBS5; Serotec), anti–human α_6 mAb (clone 4F10; Serotec). Negative and isotype controls were processed similarly. Corresponding Alexa Fluor568–labeled secondary antibodies (Molecular Probes, Leiden, the Netherlands) were used. Flow cytometry was done using EPIC XL (Beckman Coulter, Krefeld, Germany).

Static Adhesion Assays

Assays were performed in 96-well microtiter plates coated with collagen type I (C I; BD Biosciences, San Jose, CA) or fibronectin (FN; Sigma; each 10 μg/ml) as previously described [17]. Serum-starved reconstituted tumor cells (10^5) were fluorescence-labeled (CalceinAM; Molecular Probes) and added to each well in medium containing 1% BSA. This procedure was reported not to interfere with the adhesive properties of cells [17]. After the indicated adhesion time, wells were washed with phosphate-buffered saline (PBS) to remove nonadherent cells. Fluorescence is expressed as percent fluorescence of unwashed control wells. The numbers given are representative of independent triplicate experiments. t Test was used to compare groups. For adhesion assays on endothelial cells, human umbilical vein endothelial cells

(HUVECs; kindly provided by B. Löffler, Muenster) were seeded and grown confluent in 96-well dishes. Before the adhesion assay, HUVECs were activated by incubation with tumor necrosis factor α (TNF-α) (10 ng/ml; Sigma) for 12 hours. Reconstituted, fluorescence-labeled cells (10^5) were added to each well and processed as described previously.

Tumor Cell Chemotaxis

Chemotaxis was assayed in 24-well cell culture chambers (Greiner Bio One, Frickenhausen, Germany) using inserts with 8-μm pore membranes (Nunc/Thermo Fisher Scientific, Rockford, IL) coated with FN (10 μg/ml) or C I (10 mg/ml) as described [9]. Cells (2.5×10^5) were resuspended in serum-free medium containing 1% BSA and were added to the upper chamber. Serum-free medium containing CXCL12 in indicated concentrations was added to the lower chamber. After incubation for 18 hours, cells on the upper surface were removed by cotton swaps and cells on the lower surface of the membrane were fixed with ice-cold methanol and stained with hematoxylin/eosin. The membranes were removed from the inserts and mounted on microscopic slides. Cell numbers were counted using a light microscope in 16 standardized fields at an original magnification of ×16. The numbers given are means ± SD and compared by a *t* test. The numbers given are representative of three independent experiments.

Intravital Microscopy

The intravital fluorescence microscopy for evaluation of *in vivo* tumor cell adhesion and migration into the hepatic parenchyma was performed as described previously [15]. Briefly, male Sprague-Dawley rats (250-300 g; Charles River, Deisenhofen, Germany) were cared for in accordance with the standards of the German Council for Animal Care under an approved protocol of the local Animal Welfare Committee. Anesthetized animals obtained a catheter placed into the right carotid artery with the tip located central to the heart. After a wide median laparotomy, the left part of the liver was mobilized. Fluorescence microscopy was performed using an upright epifluorescence microscope (Zeiss, Jena, Germany) containing a 20-fold objective and a timer-containing S-VHS video system for further analysis (Figure 4*A*). For intravital observation of tumor cell interactions with the hepatic subcapsular microcirculation, 1×10^6 cells resuspended in 1 ml of calcium and magnesium–free PBS were injected intra-arterially as a single-cell suspension for 60 seconds. As described previously [15], this procedure did not interfere significantly with the cardiocirculatory functions of the animals. For semiquantitative analysis of cell interactions within the hepatic microcirculation, 28 microscopic fields were monitored every 5 minutes for a total of 30 minutes using a standardized procedure. The total numbers of arrested cells (adherent and migrated/extravasated) were counted, and relative migration rates were calculated as the number of migrated cells/number of arrested cells. The numbers given are means of *n* independent experiments (animals injected) for each group and groups were compared by a *t* test. Cells were harvested and prepared as described previously [17]. In some experiments, before injection, cells were incubated with a neutralizing anti-CXCR4 (MAB 173; R&D Systems), with an isotype control antibody (R&D Systems), or with CXCL12 (R&D systems) as indicated.

GTPase Activation Assay

Cells were trypsinized and reconstituted in serum-free medium containing 1% BSA for 45 minutes. After reconstitution, nonadherent cells (10^7) were treated with increasing concentrations of CXCL12 (25-500 ng/ml) or vehicle control for 15 minutes. Cells were then washed once with ice-cold PBS and lysed with 50 mM Tris-HCl buffer pH 7.4, containing 150 mM NaCl, 1% NP-40, 0.5% deoxycholate, 0.1% SDS, 5 mM EDTA, and 1 μl of inhibitor cocktail (Sigma) per 1 ml of lysis buffer. Lysates were clarified by centrifugation at 14,000*g* for 5 minutes and stored at −80°C before further processing. After protein quantitation, 30.8 μl of Rho Assay Reagent (Rhotekin RBD glutathione agarose beads; Upstate/Millipore, Eching, Germany) or 10 μl Rac/cdc42 assay reagent (PAK-1 PBD agarose conjugate; Upstate/Millipore) were added to 1000 μg of total protein and incubated for 45 minutes at 4°C. Samples were washed three times with magnesium-containing lysis buffer containing 25 mM HEPES pH 7.5, 150 mM NaCl, 1% Igepal CA-630 (Sigma), 10% glycerol, 10 mM $MgCl_2$, 1 mM EDTA, and 1 μl of inhibitor cocktail per 1 ml of lysis buffer (Upstate). The agarose beads were resuspended in 4× Laemmli sample buffer and boiled for 5 minutes. Total protein lysates were used as loading controls. The lysates were loaded on 12% polyacrylamide gels, then transferred to polyvinylidene fluoride membranes. and GTPases were finally detected with rabbit anti–RhoA antibody (Santa Cruz), mouse anti–Rac antibody (BD Biosciences Pharmingen), and rabbit anti–Cdc42 antibody (Cell Signaling, Danvers, MA). Bands were visualized with enhanced chemiluminescence (Millipore).

Atomic Force Microscopy

Tumor cells were analyzed as previously reported [19,20]. Briefly, cells were placed on a conventional glass slide and fixed with glutaraldehyde 2% in a HEPES-buffered solution. Atomic force microscopy (JPK, Nanowizard) analysis was performed by contact mode and tapping mode in fluid. The scan rate of surface imaging was less than 1 Hz, and the applied force in case of the contact mode was 0.5 nN. The spring constant of the cantilever was approximately 0.01 N·m. Images were analyzed by the software coming with the instrument. For statistical analyses, parameters at indicated time points were compared using a χ^2 test.

Results

Expression and Anatomical Localization of CXCR4 and Its Ligand CXCL12

Analysis of the chemokine receptor repertoire of tumor cells of human colon cancer cells with different liver metastatic potential revealed that tumor cells with low metastatic potential (Caco-2 and HT-29P) showed low levels of CXCR4 mRNA expression (Figure 1*A*) as well as weak cell surface expression of CXCR4 protein in 3.5% to 6.8% of tumor cells, respectively (Figure 1*A*). However, the liver metastatic subclone HT-29LMM displayed CXCR4 surface expression in 9.3% to 17.8% of the cells (Figure 1*A*). Furthermore, intracytoplasmic staining of fixed tumor cells revealed that 95% of HT-29LMM cells abundantly store CXCR4 in intracellular pools (data not shown). The most prominent cell surface expression of CXCR4 (>90%) was observed in the liver metastatic human hepatoma cell line HEP-G2 (Figure 1*A*). Flow cytometric data paralleled results obtained by quantitative real-time RT-PCR showing the most abundant CXCR4 mRNA expression in HT-29LMM and HEP-G2 cells (Figure 1*A*).

To validate the role of CXCR4 in the process of liver metastasis in patients with colorectal carcinoma, paraffin sections of primary tumors ($n = 7$) and liver metastases ($n = 38$) of colorectal carcinoma patients were analyzed for CXCR4 expression using immunohistochemistry. Six of 7 primary tumors and 27 of 38 liver metastases showed a marked

A

Cell line	Metastatic potential	CXCR4 mRNA [fg/25ng cDNA]	CXCR4 Surface-expression (Rate of positve cells)
Caco-2	non-metastatic	0.8	3.5 – 4.5%
HT-29P	low-metastatic	0.9	5.3 – 6.8%
HT-29LMM	high-metastatic	7.7	9.3 – 17.8%
HEP-G2	liver-metastatic	65.1	92.2 – 93.8%

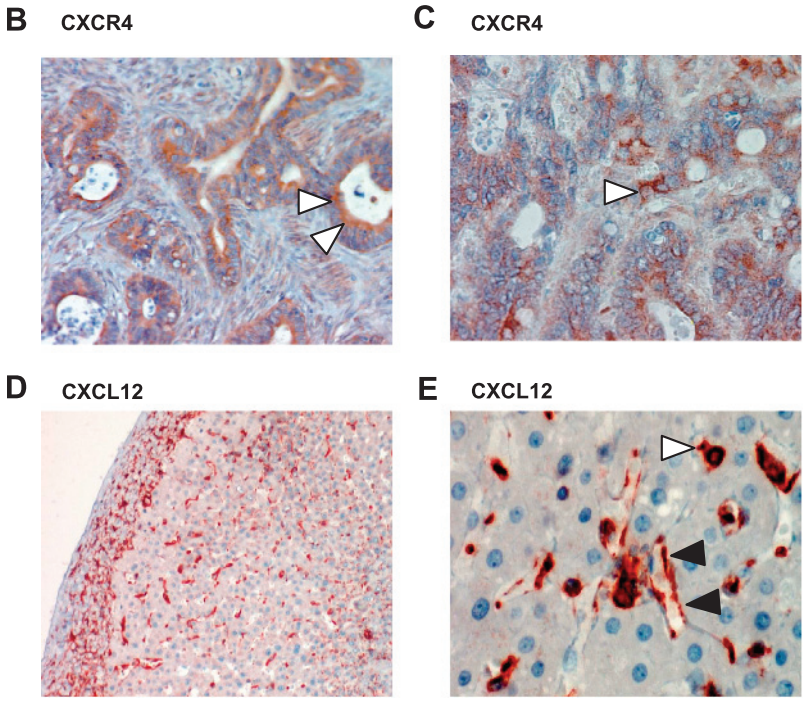

Figure 1. Metastatic human colon carcinoma cells express CXCR4 and its corresponding chemokine ligand CXCL12 is located at the interface between the sinusoidal vessel system and the liver parenchyma. (A) Cell surface as well as mRNA expression of CXCR4 by different human colon carcinoma cells (Caco-2, HT-29P, HT-29LMM) and the liver metastatic hepatocellular carcinoma cell line HEP-G2 correlates with their *in vivo* metastatic potential. Representative results of triplicate experiments. Target gene expression is presented as femtograms per 25 ng of cDNA. (B and C) Immunohistochemical evaluation of CXCR4 in a representative primary tumor (B) and liver metastasis (C) of colorectal cancer. Strong expression of CXCR4 (arrowhead) by colon cancer cells. Positive staining is indicated as red (9-amino-ethylcarbazole). Original magnification, ×100. (D and E) Immunohistochemical analysis of CXCL12 expression in normal human liver. (D) CXCL12 protein expression in the subcapsular region and sinusoidal microvessel system. Original magnification, ×40. (E) Strong CXCL12 expression is lining the inner surface of the liver sinusoids (black arrowheads) and present in disseminated cells, likely representing Kupffer cells (white arrowhead). Original magnification, ×200.

expression of CXCR4 by tumor cells (Figure 1, *B* and *C*). Moreover, dissociated single tumor cells also maintained a strong membrane as well as cytoplasmic expression of CXCR4 (data not shown).

Although we previously demonstrated that the CXCR4 ligand CXCL12 is highly expressed in human liver using quantitative real-time RT-PCR [9], it remained unclear which liver-residing cells express CXCL12 protein and where this chemokine is presented to metastatic tumor cells within the sinusoidal vessel system of the liver. Immunohistochemical analyses of normal human liver revealed that CXCL12 is expressed at the interface between the sinusoidal vessel system and the liver parenchyma (Figure 1, *D* and *E*). Sinusoidal endothelial cells lining the sinusoidal wall as well as other disseminated cells, likely representing Kupffer cells, stained positive for CXCL12 (Figure 1*E*). Thus, this chemokine is perfectly positioned to interact with circulating tumor cells during early steps of metastasis formation.

Having established that liver metastatic tumor cells express CXCR4 and that the corresponding ligand CXCL12 is readily accessible at the interface of the sinusoidal lumen and the extravascular parenchyma, we sought to investigate whether chemokine/chemokine receptor interactions play a role in tumor cell adhesion to the sinusoidal vessel wall and/or in tumor cell extravasation from the liver sinus into the liver parenchyma.

Epithelial Tumor Cell Adhesion to Extracellular Matrix and Endothelial Cells Is Independent of CXCL12/CXCR4 Interactions

Previously, we demonstrated that direct interaction of circulating tumor cells with hepatic extracellular matrix (ECM) components, such as C I and FN, within the Disse space can mediate metastatic tumor cell arrest of tumor cells within the liver [21,22]. To assess the

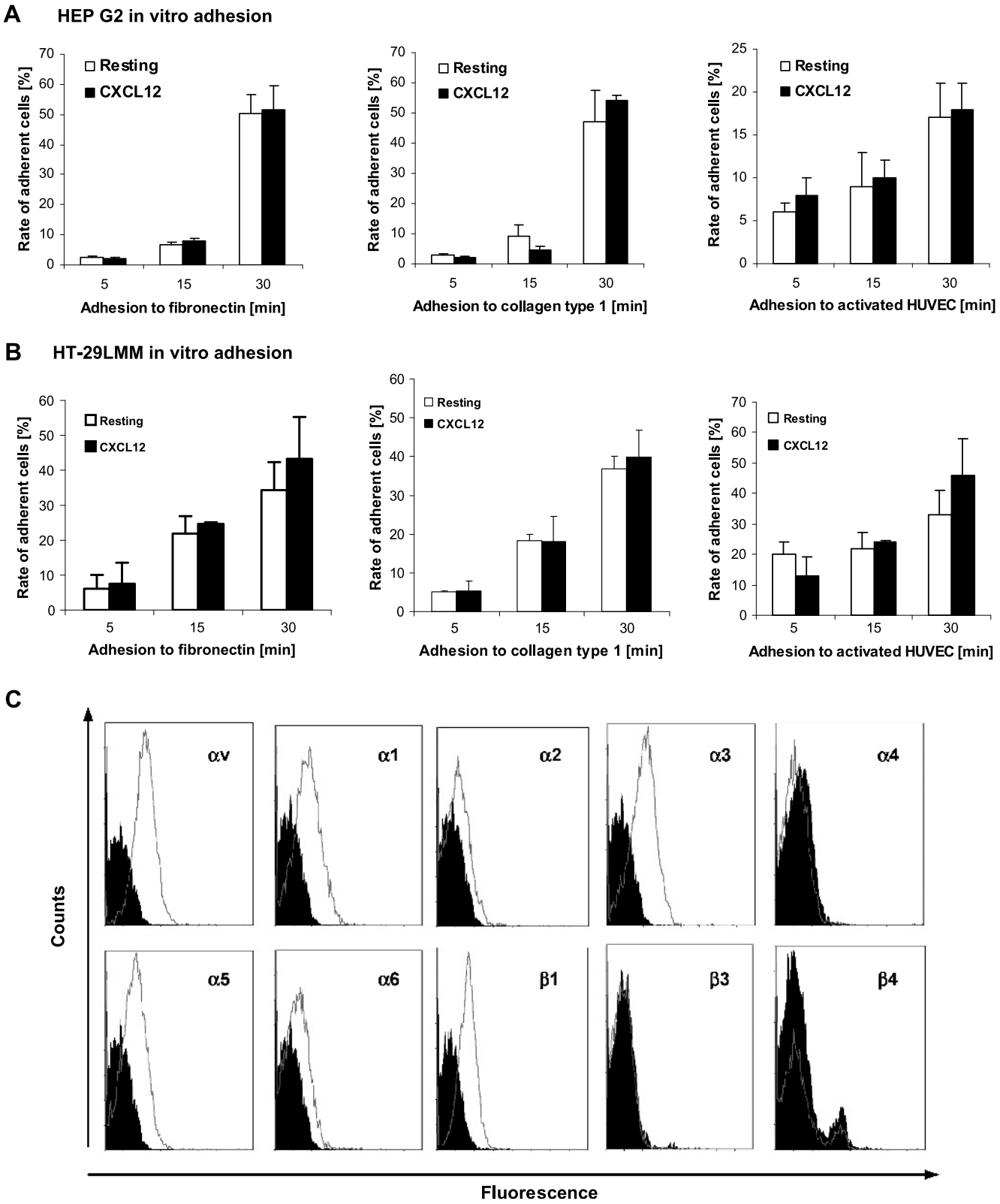

Figure 2. CXCL12 does not enhance metastatic tumor cell adhesion to ECM components present in the Disse space or to activated endothelial cells. (A and B) HEP-G2 (A) and HT-29LMM (B) cells showed time-dependent adhesion to FN and C I representing the main components of the hepatic ECM, which is readily accessible in the Disse space as well as to activated (TNF-α; 10 ng/ml for 12 hours) HUVECs. Short-term stimulation of the cells with CXCL12 (500 ng/ml for 15 minutes) did not enhance cell adhesion to these ECM components or to endothelial cells at any time interval (*t* test, $P > .05$). (D) Expression of integrin subunits by HEP-G2 cells determined by flow cytometry. Epithelial HEP-G2 tumor cells do not express the integrin α_4 subunit. Representative results of triplicate experiments are shown.

adhesive properties of HEP-G2 and HT-29LMM to these matrix proteins as the main components of the ECM of the liver [22,23], we used *in vitro* adhesion assays. HEP-G2 (Figure 2*A*) and HT-29LMM cells (Figure 2*B*) showed cell adhesion to immobilized FN or C I in a time-dependent manner (5-30 minutes). Stimulation of these cells with CXCL12 (500 ng/ml) for 15 minutes before placement on the ECM components did not change their adhesive properties *in vitro* (Figure 2, *A* and *B*). Because circulating tumor cells may also adhere to endothelial cells within the capillary system of target organs, we performed adhesion assays on TNF-α–stimulated HUVECs. CXCL12 treatment of

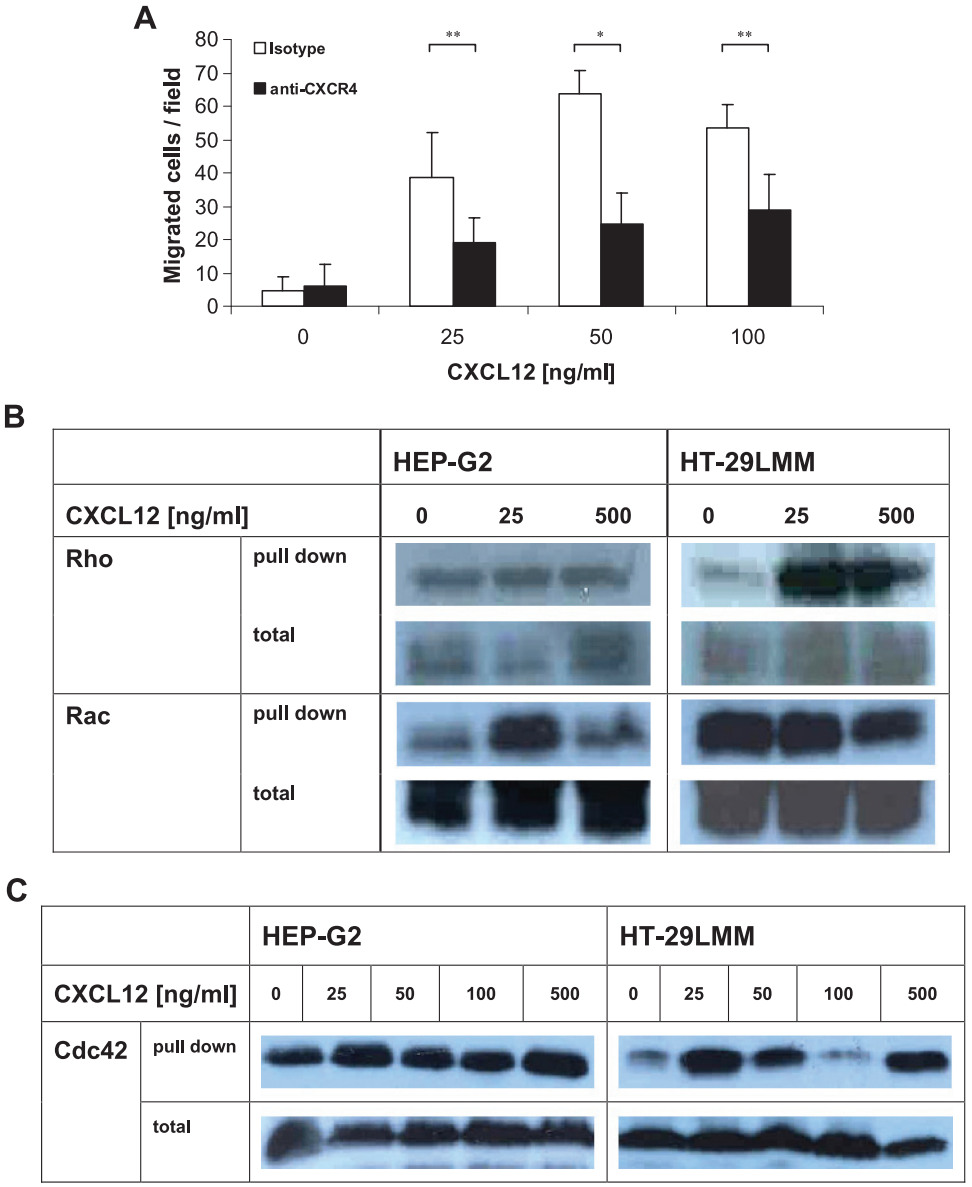

Figure 3. CXCL12/CXCR4 interaction results in the activation of small GTPases and in the induction of a migratory phenotype. (A) Chemotactic response of HEP-G2 cells to different concentrations of CXCL12 in a transwell migration assay. The migratory response is attenuated in cells treated with a neutralizing anti-CXCR4 antibody (*t* test, $*P < .05$, $**P < .001$). Representative results of triplicate experiments are shown. (B and C) In Western blot–based GTPase activation assays after short-term stimulation (15 minutes) of HEP-G2 and HT-29LMM cells with increasing concentrations of CXCL12, HEP-G2 cells showed an increased Rac activation level, whereas the Rho activity level remained unchanged. In contrast, HT-29LMM cells showed increased Rho activation, whereas Rac activity was unaffected after CXCL12 stimulation. (C) The presence of CXCL12 also induced a concentration-dependent cdc42 activation in HEP-G2 cells. In HT-29LMM cells, cdc42 activity was modulated by CXCL12 in a variable manner. Representative results of triplicate experiments are shown. (D and E) Atomic force microscopy demonstrated that tumor cells elongate and flatten their lamellipodia upon stimulation with CXCL12. The lines in the images represent the areas of measurements. (F) Determination of CXCL12-induced changes in the width of the lamellipodium of stimulated tumor cells. The width decreases from 12 to 6 μm after 10 minutes of CXCL12 stimulation with a partial recovery to a width of 10 μm after 30 minutes (χ^2 test, $P < .05$; measured 5 μm proximal from the leading edge; $n > 10$). (G) The slope of single tumor cells measured by the angle between the beginning of the lamellipodium and 3 μm proximal. Upon CXCL12 stimulation, tumor cells flattened by 12 degrees and again showed a partial recovery after 30 minutes (χ^2 test, $P < .05$; $n > 10$ for each experiment).

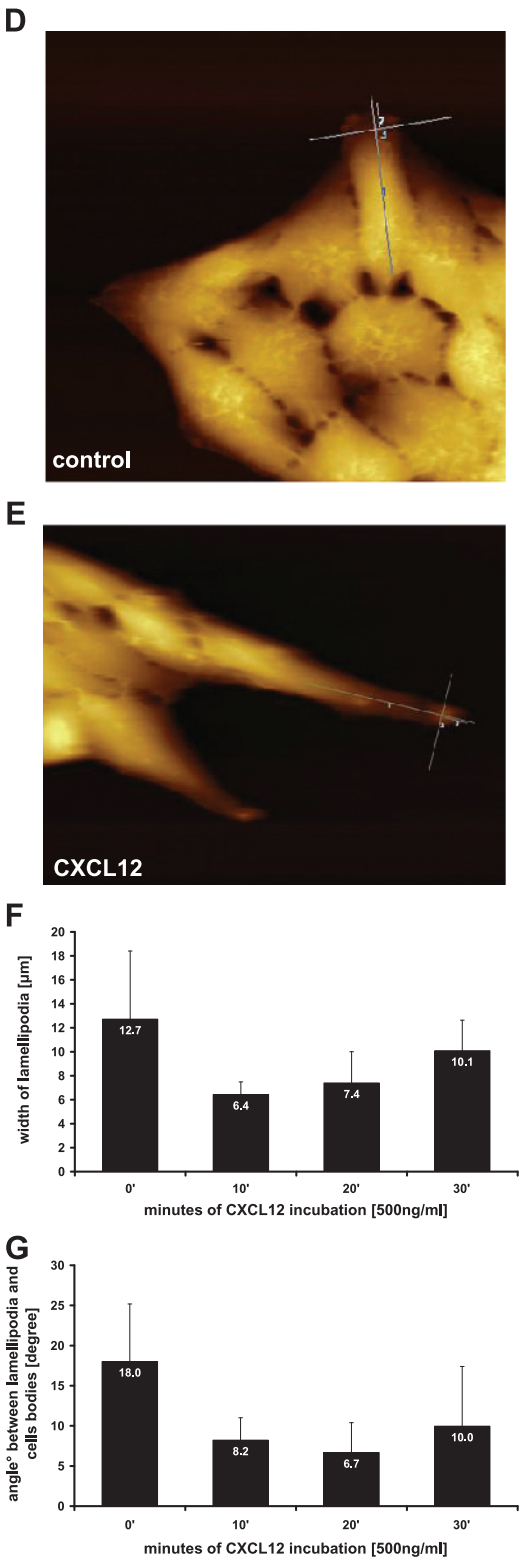

Figure 3. (*continued*).

HEP-G2 or HT-29LMM cells also did not promote their adhesion to stimulated HUVEC ($P > .05$). Only stimulated HT-29LMM showed a tendency to enhanced adhesion to HUVEC and FN after 30 minutes ($P > .05$; Figure 2, *A* or *B*).

Because increased adhesion of different tumor entities to endothelial cells through $\alpha_4\beta_1$- and $\alpha_5\beta_1$-integrins has been reported [12,24,25], we analyzed the integrin repertoire of the epithelial cancer cells used in this study. Generally, the expressed integrin repertoire enables these cells to adhere to the directly accessible ECM in the Disse space within the hepatic sinusoids [21,22]. However, integrin expression of HT-29LMM (data not shown) or HEP-G2 cells (Figure 2*D*) revealed that these liver metastatic epithelial tumor cells show only weak expression of the integrin α_5 subunit and do not express the integrin α_4 subunit that would eventually mediate adhesion to endothelial structures in a CXCL12-dependent fashion. However, HT-29LMM (data not shown) or HEP-G2 cells (Figure 2*D*) demonstrated the abundant expression of α_v-, α_2-, and α_6-integrins mediating the adhesion to FN and C I in the Disse space [21,26].

Chemokine CXCL12 Induces Tumor Cell Migration

To define the functional activity of CXCR4 expressed by tumor cells, Transwell migration assays were used. The CXCR4 ligand CXCL12 induced concentration-dependent chemotactic responses of HEP-G2 cells (Figure 3*A*). Chemotactic responses were significantly impaired in the presence of a neutralizing anti-hCXCR4 antibody indicating that CXCR4 is functionally active on HEP-G2 cells and required for CXCL12-induced directional migration (Figure 3*A*). Because chemokine receptors are known to promote chemotactic cell motility and cytoskeletal rearrangement through small GTPases, we analyzed the activation level of Rho, Rac, and cdc42 in HEP-G2 and HT-29LMM tumor cells. Both cell lines showed a specific pattern of GTPase activation in response to CXCL12 stimulation (Figure 3, *B* and *C*). Upon stimulation of HEP-G2 cells with different concentrations of CXCL12 (0, 25, 500 ng/ml), the Rho activation level was not significantly altered compared with unstimulated cells (Figure 3*B*). In contrast, the Rac activation level was increased after a low-dose stimulation with 25 ng/ml CXCL12 (Figure 3*B*). In addition, the presence of CXCL12 increased the cdc42 activation level in a concentration-dependent manner in HEP-G2 cells (Figure 3*C*).

In HT-29LMM cells, we found a slightly different pattern of GTPase activation with increasing activity of Rho upon CXCL12 stimulation up to the maximum dose of 500 ng/ml (Figure 3*B*). In contrast, no significant activation of Rac was observed at high doses (Figure 3*B*). Cdc42 activity was modulated by CXCL12 in a variable manner without stringent concentration dependency in HT-29LMM cells (Figure 3*C*).

To visualize and quantify cell morphology alterations upon chemokine stimulation, we used atomic force microscopy. Atomic force microscopy has evolved to the imaging method that yields the greatest structural details on live, biological samples. It can be used to study the three-dimensional surface topography of single cells in a physiological buffer solution. The detection limits are 10 nm for the height (*z*-axis) and approximately 100 nm for the lateral axes (*x*- and *y*-axes). In the present study, HEP-G2 tumor cells were analyzed after different periods of CXCL12 stimulation. Alterations of lamellipodia were documented by measuring the cell width and the slope of single lamellipodium. We could show that upon chemokine stimulation, single tumor cells show a flattening of their lamellipodia represented by a decrease of the cell width and a drop of the angle between the leading edge and cell body (Figure 3, *D* and *E*). These morphologic alterations could be measured already after 10 minutes of chemokine stimulation. Interestingly, after 20 and 30 minutes of stimulation, respectively, a slight recovery of the measured morphologic alterations was documented indicating a follow-up movement of the cell body (Figure 3, *F* and *G*). These data represent morphologic changes of the cells corresponding to Rac activation and

indicate that chemokine stimulation activates tumor cells within minutes to form a lamellipodium as a prerequisite to start cell migration.

CXCR4 Induces the Early Extravasation of Metastatic Tumor Cells into the Liver Parenchyma In Vivo

To evaluate the role of CXCL12/CXCR4 interactions for tumor cell adhesion and migration/extravasation *in vivo*, we used our previously described intravital fluorescence microscopy model [15,16,21] to study these initial steps during the formation of liver metastases (Figure 4*A*). This model allows the direct observation of metastatic tumor cells within the superficial sinusoidal microvessel system of the liver. The number of arrested cells within the liver sinusoids (Figure 4*B*) and the relative numbers of extravasated/migrated cells (Figure 4*C*) were quantified *in vivo*. Previously, we confirmed the early extravasation of tumor cells using three-dimensional laser scanning microscopy [16].

Because liver metastatic HEP-G2 and HT-29LMM cells showed the highest expression of CXCR4 *in vitro*, these tumor cell lines were chosen for further intravital fluorescence microscopy experiments. Tables of the supplemental material give detailed numbers and statistics of *in vivo* cell adhesion and extravasation for HEP-G2 (Table W1) and HT-29LMM cells (Table W2).

The total number of arrested untreated HEP-G2 (n = 13 independent experiments), isotype control-treated HEP-G2 (n = 8 independent experiments), and isotype control-treated HT-29LMM (n = 8 independent experiments) cells reached 55.4 ± 14.6, 44.2 ± 3.2, and 59.0 ± 11.8 cells/28 microscopic fields, respectively, within 30 minutes after tumor cell injection (Figure 4, *F*, *D*, and *H*). The rates of early tumor cell extravasation/migration of untreated HEP-G2 (n = 13 independent experiments), isotype control-treated HEP-G2 (n = 8 independent experiments), and isotype control treated HT-29LMM (n = 8 independent experiments) cells reached 18% ± 11%, 22% ± 4%, and 9% ± 3%, respectively, of all arrested cells within 30 minutes after tumor cell injection (Figure 4, *G*, *E*, and *I*). To determine the functional role of CXCR4 for adhesion and extravasation/migration of metastatic tumor cells *in vivo*, HEP-G2 cells were treated with a neutralizing anti–human CXCR4 antibody before injecting into Sprague-Dawley rats (n = 12 independent experiments). Most interestingly, blocking of CXCR4 signaling did not affect the adherence of tumor cells within the hepatic microcirculation (isotype control: 44.2 ± 3.4 cells/28 microscopic *vs* anti-CXCR4: 49.4 ± 24.8 cells/28 microscopic; P = .184; Figure 4*D*); however, the rates of migrated/extravasated cells were significantly decreased from a maximum of 22% ± 4% in the isotype-treated group to 6% ± 5% after anti-hCXCR4 treatment (P < .001; Figure 4*E*). Using liver metastatic human HT-29LMM colon cancer cells, blocking of CXCR4 (n = 8 independent experiments) resulted in a slightly reduced adhesion that did not reach a significant level at all time intervals (Figure 4*H*), but extravasation of HT-29LMM was significantly impaired after inhibition of CXCR4 (Figure 4*I*).

To investigate whether CXCL12 can induce a "specific" extravasation program in tumor cells, we stimulated tumor cells with CXCL12 protein (500 ng/ml) for 15 minutes before *in vivo* injection. In fact, CXCL12 treatment did not affect the adherence of HEP-G2 (n = 7 independent experiments; Figure 4*F*) or HT-29LMM cells (n = 9 independent experiments; Figure 4*I*) to the vessel wall of the liver sinusoids *in vivo* but significantly enhanced the rates of extravasated cells to a maximum of 41% ± 3% compared with 18% ± 11% of vehicle-treated HEP-G2 cells (P < .001; Figure 4*G*). Comparing the migration rates of isotype control-treated and CXCL12-treated cells, similar results were observed for HT-29LMM between 15 and 30 minutes after cell injection (Figure 4*I*). At the end of the observation period, the rate of extravasated isotype control-treated HT-29LMM cells was significantly lower with 9% ± 3% compared with 20% ± 8% of CXCL12-treated cells (P = .003).

Taken together, intravital fluorescence videomicroscopy analyses identified for the first time CXCR4-independent adhesion, but CXCL12/CXCR4 triggered extravasation of metastasizing tumor cells in the early phase of liver colonization.

Discussion

Colorectal cancer shows a high prevalence of liver metastasis and the clinical course of hepatocellular carcinoma is frequently dominated by intrahepatic metastasis [27]. For example, after liver transplantation, recurrence of hepatocellular carcinoma within the transplanted liver likely reflects an organ-specific homing of circulating tumor cells into the allograft [28]. Previous studies demonstrated a role for the chemokine receptor CXCR4 in the dissemination of colorectal cancer to the liver [13], in local and systemic progression of hepatocellular carcinoma [14], as well as in metastasis formation of other tumor entities [29,30]. However, the precise mechanisms of chemokine-mediated liver metastasis formation remained elusive.

Migratory and adhesive properties of tumor cells are critical parameters for the development of metastasis [31]. We previously demonstrated that CXCR4 can mediate directional migration and metastasis of human breast cancer cells [9]. Although the CXCR4 ligand CXCL12 is highly expressed within human liver using quantitative real-time RT-PCR [9], it remained unclear which liver-residing cells express CXCL12 protein and where this chemokine is presented to metastatic tumor cells within the sinusoidal vessel system of the liver. Immunohistochemical analyses of normal human liver specimens revealed that CXCL12 is expressed at the interface between the sinusoidal vessel system and the liver parenchyma. Sinusoidal endothelial cells lining the microvascular hepatic vessel wall, as well as disseminated cells, likely representing Kupffer cells, abundantly presented CXCL12 protein. Thus, this chemokine is perfectly positioned to interact with circulating tumor cells during early steps of metastasis formation.

To investigate the mechanisms of chemokine receptor–mediated events during early phases of metastasis *in vivo*, we monitored the interactions of tumor cells with the microvessel system of the liver sinusoids by intravital fluorescence microscopy [15]. Taking advantage of this model, we previously reported that tumor cells with different liver metastatic potential showed no significant differences in adhesion to liver sinusoids [16]. In contrast to their adhesive properties, the ability of tumor cells to extravasate into the liver parenchyma correlated with their metastatic potential [16]. In the present study, inhibition of CXCR4 signaling of colorectal cancer and hepatocellular carcinoma cells showed unaffected adhesion within the hepatic microvasculature *in vivo*, but tumor cell extravasation was significantly impaired after blockade of CXCR4 signaling. In corresponding *in vivo* experiments, stimulation of tumor cells with CXCL12 accelerated migration/extravasation but did not affect adhesion to endothelial cells or ECM components.

Taken together, intravital fluorescence videomicroscopy analyses identified for the first time that liver metastatic epithelial tumor cells exhibit CXCR4-independent adhesive properties *in vivo* but demonstrate CXCR4-regulated extravasation into the liver parenchyma upon interaction with its specific ligand CXCL12.

These results were surprising because enhanced tumor cell adhesion to endothelial cells because of CXCL12 treatment was reported for other

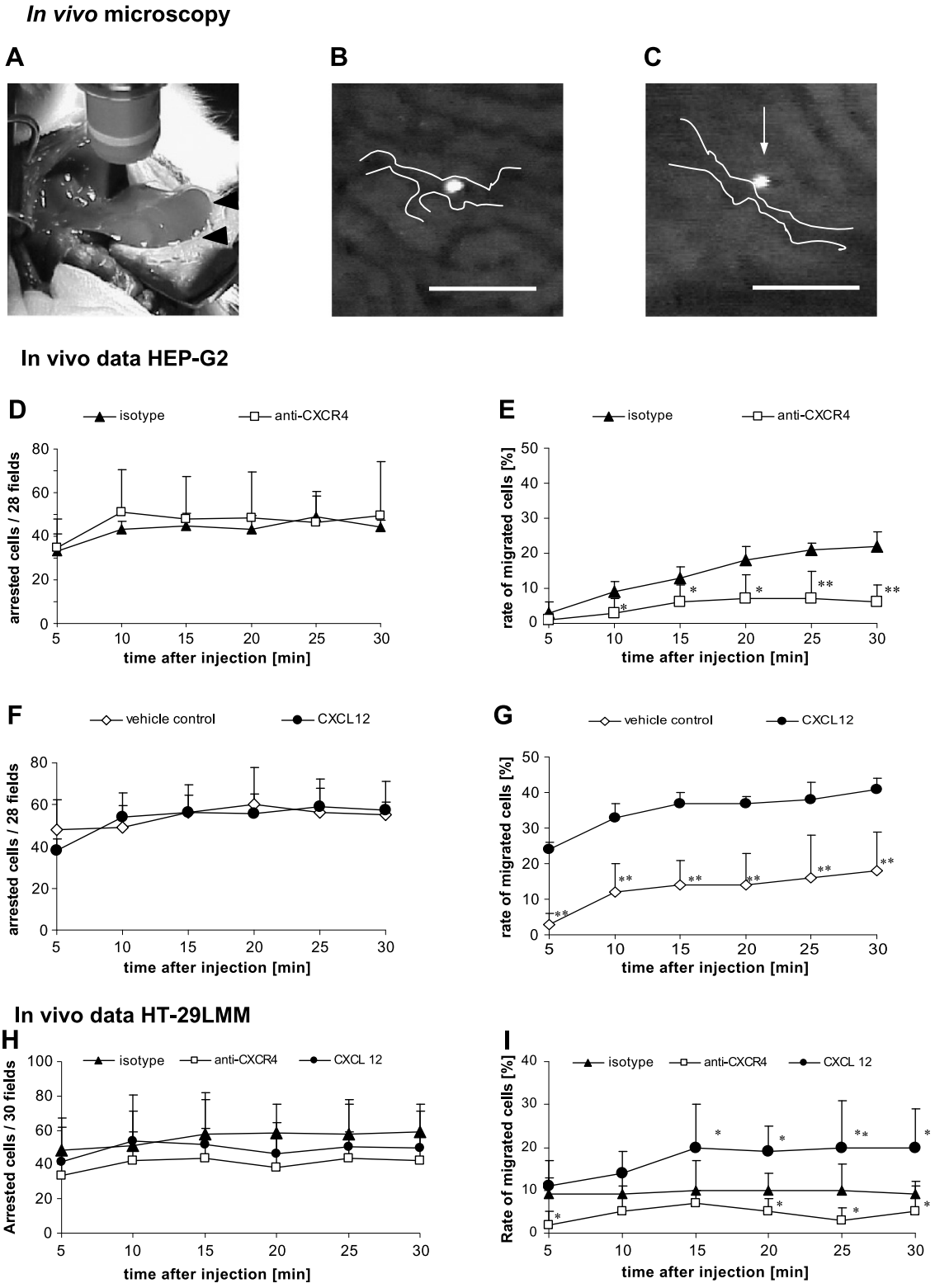

Figure 4. CXCL12/CXCR4 interactions promote early extravasation of metastatic tumor cells *in vivo*. (A–C) Intravital microscopy setup. A median laparotomy was performed in anesthetized rats. The left part of the liver lobe (arrows) is carefully mobilized and positioned under an upright fluorescence microscope for an observation period of 30 minutes. (B and C) After injection of 10^6 fluorescence-labeled tumor cells into the left ventricle, cells enter the sinusoidal vessel system, become adherent to the sinusoidal wall (B; sinusoidal wall outlined), and extravasate (C; sinusoidal wall outlined). Scale bars, 50 μm. Adhesion and migration are quantified using a standardized procedure. (D and E) CXCR4 neutralization did not impair tumor cell adhesion to the sinusoidal wall (D) but significantly impaired extravasation of HEP-G2 cells into the liver parenchyma *in vivo* (E). (F and G) Treatment of tumor cells with the CXCR4 ligand CXCL12 before injection did not affect cell adhesion within the liver sinusoids (F) but facilitated tumor extravasation (G). (H and I) Using HT-29LMM cells too, CXCR4 neutralization or CXCR4 stimulation did not affect tumor cells adhesion to the sinusoidal wall (H). In contrast, CXCR4 neutralization impaired, and CXCR4 stimulation by its ligand CXCL12 facilitated tumor cell extravasation (I). *$P < .05$; **$P < .001$.

tumor entities, such as small cell lung cancer, myeloma, and melanoma cells [12,24,25]. Nonepithelial tumor cell adhesion to endothelial cells and ECM was mainly mediated by $\alpha_4\beta_1$-integrins and partly by $\alpha_5\beta_1$-integrins, respectively [12]. Upon chemokine stimulation, $\alpha_4\beta_1$-integrin avidity and affinity were increased [12,24], and Arg-Gly-Asp–dependent adhesion to FN or laminin was stimulated [32]. In breast cancer cells, facilitated phosphorylation of focal adhesion kinase and increased adhesion to FN after CXCL12 stimulation were reported [33]. Because HT-29LMM and HEP-G2 cells do not express the integrin α_4 subunit and show only weak expression of the integrin α_5 subunit, their adhesion to the endothelium cannot be mediated by α_4-integrins but seems to be mainly mediated by CXCR4-independent systems such as sialylated glycoproteins or Thomson-Friedenreich glycoantigen as ligands for endothelial selectins [21,34] and galectin-3 [35], respectively. In contrast, migration of carcinoma cells along C I bundles reaching from the subendothelial Disse space into the interstitium between hepatocytes appears to be an important property for metastatic extravasation into the liver [22]. CXCL12 was shown to accelerate undirected cancer cell motility [36] as well as inducing directed chemotaxis of epithelial cancer cells [37]. Here, we show for the first time that the CXCR4 ligand CXCL12 is presented to adhering tumor cells by the endothelium lining the sinusoidal vessel wall and by Kupffer cells. Furthermore, chemokines, such as CXCL12, can also be presented by ECM proteins [38] that are directly accessible in the sinusoids for adhering cells [21].

Chemokine receptor– and other G protein–coupled receptor–meditated induction of cell motility is critically dependent on the activation of small GTPases such as the Rho family. RhoA and RhoC promote the formation of actin stress fibers and the generation of contractile forces, whereas Rac was found to promote the formation of lamellipodia. Cdc42 is associated with the formation of microspikes to sense chemotactic gradients. In osteosarcoma cells, chemokine-induced cell migration involves RhoA signaling, which seems to be critically involved in experimental metastasis [39]. In contrast, in breast cancer cells, Rac and cdc42 promote migration and invasion in a Rho-independent manner [40]. Using sarcoma cells, other reports [41] indicated that invasive cancer cells can use different modes of cell migration depending on the type of activated GTPases. Whereas Rho activation promoted tumor cell invasion as an ameboid migration phenotype, Rac activation resulted in the invasion as elongated cells. These results indicate that activation of either Rho or Rac can induce tumor cell invasion depending on the cell type and the surrounding conditions that are determined by the microenvironment of metastatic target organs. In the present study, CXCL12 stimulation resulted in Rho activation in HT-29LMM colon cancer cells and in Rac activation and lamellipodia formation in HEP-G2 hepatoma cells. Nevertheless, both pathways, through Rho or Rac, seem sufficient in mediating CXCR4 signaling and inducing cell migration as well as extravasation *in vivo*. In both cell lines, CXCL12-induced cdc42 activity may have facilitated the sensing of chemotactic gradients within the hepatic sinusoids and thereby act synergistically with Rho or Rac to promote tumor cell extravasation within the liver.

Taken together, intravital fluorescence microscopy allowed us to dissect the early steps of liver metastases formation. The chemokine CXCL12 is ideally positioned at the interface between the sinusoids and the liver parenchyma to interact with circulating, metastatic, and CXCR4-expressing tumor cells. Furthermore, sequestering of CXCL12 through binding to FN or glycosaminoglycans [38] that are present in the Disse space may also support CXCL12/CXCR4–induced tumor cell extravasation from the liver sinuses into the parenchyma. Nevertheless, CXCL12/CXCR4 interactions obviously do not favor adhesion of epithelial cancer cells to the endothelium or to ECM components within the liver. CXCL12/CXCR4 interactions promote early extravasation of liver metastatic epithelial cancer cells and can thereby determine a critical step in organ-specific metastases formation. Understanding these mechanisms is of particular importance because a variety of small molecule antagonists against chemokine receptors, including CXCR4, are currently under preclinical or clinical evaluation and may be available for the treatment of cancer patients in the years to come.

Acknowledgments

The authors thank Petra Franken-Kunkel and Katja Hagen for excellent technical assistance.

References

[1] Chambers AF, Groom AC, and Macdonald IC (2002). Dissemination and growth of cancer cells in metastatic sites. *Nat Rev Cancer* **2**, 563–572.

[2] Yeatman TJ and Nicolson GL (1993). Molecular basis of tumor progression: mechanisms of organ-specific tumor metastasis. *Semin Surg Oncol* **9**, 256–263.

[3] Zlotnik A and Yoshie O (2000). Chemokines. A new classification system and their role in immunity. *Immunity* **12**, 121–127.

[4] Campbell JJ and Butcher EC (2000). Chemokines in tissue-specific and microenvironment-specific lymphocyte homing. *Curr Opin Immunol* **12**, 336–341.

[5] Youngs SJ, Ali SA, Taub DD, and Rees RC (1997). Chemokines induce migrational responses in human breast carcinoma cell lines. *Int J Cancer* **71**, 257–266.

[6] Robledo MM, Bartolome RA, Longo N, Rodriguez-Frade JM, Mellado M, Longo I, van Muijen GNP, Sanchez-Meteos P, and Teixido J (2001). Expression of functional chemokine receptors CXCR3 and CXCR4 on human melanoma cells. *J Biol Chem* **276**, 45098–45105.

[7] Rubin JB, Kung AL, Klein RS, Chan JA, Sun Y, Schmidt K, Kieran MW, Luster AD, and Segal RA (2003). A small molecule antagonist of CXCR4 inhibits intracranial growth of primary brain tumors. *Proc Natl Acad Sci USA* **100**, 13513–13518.

[8] Chen Y, Stamatoyannopoulo G, and Song CZ (2003). Down regulation of CXCR4 by inducible small interfering RNA inhibits breast cancer cell invasion *in vitro*. *Cancer Res* **63**, 4801–4804.

[9] Müller A, Homey B, Soto H, Ge N, Catron D, Buchanan ME, McClanahan T, Murphy E, Yuan W, Wagner S, et al. (2001). Involvement of chemokine receptors in breast cancer metastases. *Nature* **410**, 50–56.

[10] Murakami T, Maki W, Cardones AR, Fang H, Kyi AT, Nestle FO, and Hwang ST (2002). Expression of CXC chemokine receptor-4 enhances the pulmonary metastatic potential of murine B16 melanoma cells. *Cancer Res* **62**, 7328–7334.

[11] Bertolini F, Dell'Agnola C, Mancuso P, Rabascio C, Alessandra B, Monestiroli S, Gobbi A, Pruneri G, and Martinelli G (2002). CXCR4 neutralization, a novel therapeutic approach for non–Hodgkin's lymphoma. *Cancer Res* **62**, 3106–3112.

[12] Cardones AR, Murakami T, and Hwang ST (2003). CXCR4 enhances adhesion of B16 tumor cells to endothelial cells *in vitro* and *in vivo* via α_1 integrin. *Cancer Res* **63**, 6751–6757.

[13] Kim J, Mori T, Chen SL, Amersi FF, Martinez SR, Kuo C, Turner RR, Ye X, Bilchik AJ, Morton DL, et al. (2006). Chemokine receptor CXCR4 expression in patients with melanoma and colorectal cancer liver metastases and the association with disease outcome. *Ann Surg* **244**, 113–120.

[14] Schimanski CC, Bahre R, Gockel I, Müller A, Frerichs K, Hörner V, Teufel A, Simiantonaki N, Biesterfeld S, Wehler T, et al. (2006). Dissemination of hepatocellular carcinoma is mediated via chemokine receptor CXCR4. *Br J Cancer* **95**, 210–217.

[15] Haier J, Korb T, Hotz B, Spiegel HU, and Senninger N (2003). An intravital model to monitor steps of metastatic tumor cell adhesion within the hepatic microcirculation. *J Gastrointest Surg* **7**, 507–514.

[16] Schlüter K, Gassmann P, Enns A, Korb T, Hemping-Bovenkerk A, Hölzen JP, and Haier J (2006). Organ-specific metastatic tumor cell adhesion and extravasation of colon carcinoma cells with different metastatic potential. *Am J Pathol* **169**, 1064–1073.

[17] Haier J, Nasralla M, and Nicolson GL (1999). Different adhesion properties of highly and poorly metastastic HT-29 colon carcinoma cells with extracellular

matrix components: role of integrin expression and cytoskeletal components. *Br J Cancer* **80**, 1867–1874.

[18] Homey B, Wang W, Soto H, Buchanan ME, Wiesenborn A, Catron D, Müller A, McClanahan TK, Dieu-Nosjean MC, Orozco R, et al. (2000). Cutting edge: the orphan chemokine receptor G protein–coupled receptor-2 (GPR-2, CCR10) binds the skin-associated chemokine CCL27 (CTACK/ALP/ILC). *J Immunol* **164**, 3465–3470.

[19] Schneider SW, Sritharan CK, Geibel JP, Oberleithner H, and Jena BP (1997). Surface dynamics in living acinar cells imaged by atomic force microscopy: identification of plasma membrane structures involved in exocytosis. *Proc Natl Acad Sci USA* **94**, 316–321.

[20] Schneider SW, Matzke R, Radmacher M, and Oberleithner H (2004). Shape and volume of living aldosterone-sensitive cells imaged with atomic force microscopy. *Methods Mol Biol* **242**, 255–279.

[21] Enns A, Gassmann P, Schlueter K, Korb T, Spiegel HU, Senninger N, and Haier J (2004). Integrins can directly mediate metastatic tumor cell adhesion within liver sinusoides. *J Gastrointest Surg* **8**, 1049–1059.

[22] Rosenow F, Ossig R, Thormeyer D, Gassmann P, Schlüter K, Brunner G, Haier J, and Eble JA (2008). Integrins as antimetastatic targets of RGD-independent snake venom components in liver metastasis [corrected]. *Neoplasia* **10**, 168–176; Erratum in: Neoplasia. 10:410.

[23] Martinez-Hernendez A and Amenta PS (1993). The hepatic extracellular matrix. I. Components and distributionin normal liver. *Virchows Arch A Pathol Anat Histopathol* **423**, 1–11.

[24] Burger M, Glodek A, Hartmann T, Schmitt-Gräf A, Silberstein LE, Fuji N, Kipps TJ, and Burger JA (2003). Functional expression of CXCR 4 (CD184) on small-cell lung cancer cells mediates migration, integrin activation, and adhesion to stromal cells. *Oncogene* **22**, 8093–8101.

[25] Parmo-Carbanas M, Bartolome RA, Wright N, Hidalgo A, Drager AM, and Teixido J (2004). Integrin $\alpha_4\beta_1$ involvement in stromal cell–derived factor-1α–promoted myeloma cell transendothelial migration and adhesion: role of cAMP and the actin cytoskeleton in adhesion. *Exp Cell Res* **294**, 571–580.

[26] Enns A, Korb T, Schlüter K, Gassmann P, Spiegel HU, Senninger N, Mitjans F, and Haier J (2005). $\alpha_v\beta_5$-Integrins mediate early steps of metastasis formation. *Eur J Cancer* **41**, 1065–1072.

[27] Poston GJ (2004). Surgical strategies for colorectal liver metastases. *Surg Oncol* **13**, 125–136.

[28] Schlitt HJ, Neipp M, Weimann A, Oldhafer KJ, Schmoll E, Boecker K, Nashan B, Kubicka S, Maschek H, Tusch G, et al. (1999). Recurrence patterns of hepatocellular and fibrolamellar carcinoma after liver transplantation. *J Clin Oncol* **17**, 324–331.

[29] Akashi T, Koizumi K, Tsuneyama K, Saiki I, Takano Y, and Fuse H (2008). Chemokine receptor CXCR4 expression and prognosis in patients with metastatic prostate cancer. *Cancer Sci* **99**, 539–542.

[30] Yasumoto K, Koizumi K, Kawashima A, Saitoh Y, Arita Y, Shinohara K, Minami T, Nakayama T, Sakurai H, Takahashi Y, et al. (2006). Role of the CXCL12/CXCR4 axis in peritoneal carcinomatosis of gastric cancer. *Cancer Res* **66**, 2181–2187.

[31] Price JT and Thompson EW (2002). Mechanisms of tumour invasion and metastasis: emerging targets for therapy. *Expert Opin Ther Targets* **6**, 217–233.

[32] Libura J, Drukala J, Majka M, Tomescu O, Navenot JM, Kucia M, Marquez L, Peiper SC, Barr FC, Janowska-Wieczorek A, et al. (2002). CXCR4-SDF-1 signaling is active in rhabdomyosarcoma cells and regulates locomotion, chemotaxis, and adhesion. *Neoplasia* **100**, 2597–2606.

[33] Fernandis AZ, Prasad A, Band H, Klösel R, and Ganju RK (2004). Regulation of CXCR4-mediated chemotaxis and chemoinvasion of breast cancer cells. *Oncogene* **23**, 157–167.

[34] Witz IP (2006). Tumor-microenvironment interactions: the selectin-selectin ligand axis in tumor-endothelium cross talk. *Cancer Treat Res* **130**, 125–140.

[35] Glinskii OV, Huxley VH, Glinsky GV, Pienta KJ, Raz A, and Glinsky VV (2005). Mechanical entrapment is insufficient and intercellular adhesion is essential for metastatic cell arrest in distant organs. *Neoplasia* **7**, 522–527.

[36] Kucia M, Jankowski K, Reca R, Wysoczynski M, Bandura L, Allendorf DJ, Zhang J, Ratajczak J, and Ratajczak MZ (2004). CXCR4–SDF-1 signalling, locomotion, chemotaxis and adhesion. *J Mol Histol* **35**, 233–245.

[37] Koshiba T, Hosotani R, Miyamoto Y, Ida J, Tsuji S, Nakajima S, Kawaguchi M, Kobayashi H, Doi R, Hori T, et al. (2000). Expression of stromal cell–derived factor 1 and CXCR4 ligand receptor system in pancreatic cancer: a possible role for tumor progression. *Clin Cancer Res* **6**, 3530–3535.

[38] Pelletier AJ, van der Laan LJW, Hildbrand P, Siani MA, Thompson DA, Dawson PE, Torbett BE, and Salomon DR (2000). Presentation of chemokine SDF-1α by fibronectin mediates directed migration of T cells. *Blood* **96**, 2682–2690.

[39] Miyoshi K, Wakioka T, Nishinakamura H, Kamio M, Yang L, Inoue M, Hasegawa M, Yonemitsu Y, Komiya S, and Yoshimura A (2004). The Sprouty-related protein Spred, inhibits cell motility, metastasis and Rho-mediated actin reorganisation. *Oncogene* **23**, 5567–5576.

[40] Keely PJ, Westwick JK, Whitehead IP, Der CJ, and Parise LV (1997). Cdc42 and Rac1 induce integrin-mediated cell motility and invasiveness through PI(3)K. *Nature* **390**, 632–636.

[41] Sahai E and Marshall CJ (2003). Differing modes of tumour cell invasion have distinct requirements for Rho/ROCK signalling and extracellular proteolysis. *Nat Cell Biol* **5**, 711–719.

Table W1. *In Vivo* Adhesion and Extravasation of HEP-G2.

HEP-G2	*In Vivo*	Time Interval After Cell Injection (min)					
		0-5	6-10	11-15	16-20	21-25	26-30
Untreated, vehicle control (n = 13)	Adhesion ± SD (cells/28 microscopic fields)	47.9 ± 15.2	49.4 ± 17.5	56.1 ± 12.8	60.0 ± 19.2	56.4 ± 15.1	55.4 ± 14.6
	Extravasation (%)	3.0 ± 3.1	12.5 ± 8.2	14.1 ± 7.3	14.0 ± 8.8	16.2 ± 12.3	18.3 ± 11.5
IgG 2b isotype control (n = 8)	Adhesion ± SD (cells/28 microscopic fields)	33.3 ± 8.0	43.0 ± 4.0	44.8 ± 5.7	43.4 ± 5.9	48.7 ± 11.9	44.2 ± 3.4
	Extravasation (%)	2.9 ± 3.1	9.1 ± 2.8	12.9 ± 2.9	18.3 ± 4.3	20.6 ± 2.3	22.3 ± 4.3
Anti-CXCR4 (n = 12)	Adhesion ± SD (cells/28 microscopic fields)	34.9 ± 13.0	51.2 ± 19.5	48.0 ± 19.3	48.4 ± 21.0	46.2 ± 12.1	49.4 ± 24.8
	Extravasation (%)	1.0 ± 2.4	3.3 ± 4.0	6.2 ± 5.4	7.0 ± 6.9	7.4 ± 8.2	6.0 ± 5.0
CXCL12 (n = 9)	Adhesion ± SD (cells/28 microscopic fields)	38.0 ± 6.8	54.3 ± 7.7	56.3 ± 12.8	55.9 ± 14.8	58.9 ± 13.7	57.6 ± 6.1
	Extravasation (%)	23.5 ± 2.4	32.7 ± 3.5	36.5 ± 2.9	37.1 ± 2.1	38.1 ± 5.1	40.6 ± 3.5
t Test (P)							
IgG 2b isotype *vs* anti-CXCR4	Adhesion	.639	.153	.368	.200	.467	.184
	Extravasation	.092	.002	.005	.001	<.001	<.001
IgG 2b isotype *vs* CXCL12	Adhesion	.121	.489	.972	.632	.717	.717
	Extravasation	<.001	<.001	<.001	<.001	<.001	<.001

Table displays detailed results and statistics of tumor cell adhesion and extravasation *in vivo* using HEP-G2. Relative migration/extravasation rates were calculated as percentage of cells localized within the liver parenchyma in relation to the total number of arrested cells.

Table W2. *In Vivo* Adhesion and Extravasation of HT-29LMM.

HT-29LMM	*In Vivo*	Time Interval After Cell Injection (min)					
		0-5	6-10	11-15	16-20	21-25	26-30
IgG 2b isotype control (n = 8)	Adhesion ± SD (cells/28 microscopic fields)	48.2 ± 13.3	51.0 ± 20.2	57.7 ± 23.9	58.5 ± 16.8	57.5 ± 20.3	59.0 ± 11.8
	Extravasation (%)	8.7 ± 4.3	9.4 ± 4.8	9.8 ± 7.1	10.1 ± 4.0	10.0 ± 6.4	8.7 ± 2.5
Anti-CXCR4 (n = 12)	Adhesion ± SD (cells/28 microscopic fields)	33.3 ± 13.0	42.3 ± 16.7	43.9 ± 17.3	38.4 ± 16.6	43.7 15.3	42.1 ± 14.3
	Extravasation (%)	2.2 ± 3.3	5.0 ± 5.8	6.5 ± 2.6	5.4 ± 2.6	3.0 ± 3.2	4.7 ± 5.8
CXCL12 (n = 9)	Adhesion ± SD (cells/28 microscopic fields)	41.4 ± 25.5	53.4 ± 26.9	51.9 ± 25.6	46.5 ± 18.8	50.4 ± 24.8	49.5 ± 25.7
	Extravasation (%)	11.2 ± 5.5	14.1 ± 5.2	20.1 ± 9.7	19.1 ± 5.7	20.0 ± 11.3	19.7 ± 8.5
t Test (P)							
IgG 2b isotype *vs* anti-CXCR4	Adhesion	.039	.364	.207	.030	.147	.022
	Extravasation	.005	.116	.234	.013	.015	.092
IgG 2b isotype *vs* CXCL12	Adhesion	.511	.839	.636	.175	.529	.354
	extravasation	.317	.069	.027	.002	.043	.003

Table displays detailed results and statistics of tumor cell adhesion and extravasation *in vivo* using HT-29LMM. Relative migration/extravasation rates were calculated as percentage of cells localized within the liver parenchyma in relation to the total number of arrested cells.